AIAA JOURNAL
Vol. 38, No. 9, September 2000

Effects of Wall Admittance Changes on Aeroelastic Stability of Turbomachines

Xiaofeng Sun* and Shojiro Kaji†
University of Tokyo, Tokyo 113, Japan

In the present investigation a kind of new lifting surface model has been suggested based on the application of generalized Green's function theory and double Fourier transformation technique, which is suitable for supersonic cascade with subsonic leading-edge locus. The theoretical analysis shows that the change of wall boundary condition not only affects the eigenvalues of the system but also the eigenfunction normalizing factor in comparison with a rigid boundary condition, and it is these variations that affect the flow and acoustic field. On the other hand, through the present numerical simulation the change of wall admittance leads to very remarkable effects on both the lift and moment coefficients, which will determine whether a nonrigid wall has a positive effect on suppressing blade flutter or not. This means that if one aims at suppressing cascade flutter by use of a nonrigid wall one of the best ways is to find soft wall with a controllable acoustic admittance.

Nomenclature

A_{ab} = periphery of a blade
A_b = upper or lower surface of a blade
b = blade semichord
C_{Fqi}, $C_{F\alpha i}$ = imaginary part of blade lift coefficient
C_{Fqr}, $C_{F\alpha i}$ = real part of blade lift coefficient
C_{Mqi}, $C_{M\alpha i}$ = imaginary part of blade moment coefficient
C_{Mqr}, $C_{M\alpha r}$ = real part of blade moment coefficient
H = height from the hub to the tip side
h = height from the hub to the tip side in the transformed space
h_1 = stagger distance, measured parallel to chord
h_2 = gap distance, measured normal to chord
i = $\sqrt{-1}$
k_b = wave number, $k_b = \omega_b / a_0$
M_t = blade circumferential Mach number in mean radius
M_x = Mach number in x' direction
M_y = Mach number in negative y' direction
$\bar{p}_m$ = amplitude of perturbation pressure for mth blade
t = time in an observer point
U = mean velocity
U_r = mean velocity in chordwise direction
V = mean velocity in negative y' direction
V_n = normal velocity of a body boundary
$\bar{v}$ = upwash velocity of the reference blade
x, y, z = blade-fixed coordinate system for an observer
x_0, y_0, z_0 = blade-fixed coordinate system for a source
x', y', z' = duct-fixed coordinate system
α = wave number in ξ direction
β = wave number in η direction
β_a = wall admittance
$\Delta \bar{p}_m$ = amplitude of pressure difference for the mth blade
η_z = independent variable of wall admittance
η_{0m} = source coordinate for the mth blade
θ = blade stagger angle
Λ_h, Λ_s, Λ_v = eigenfunction normalizing factor
λ = reduced frequency based on blade chord
ξ, η, ζ = blade-fixed coordinate system for an observer in the transformed space
ξ_p = particle displacement
ξ_{pa} = amplitude of particle displacement
ξ_{pi} = particle displacement inside the surface of a liner
ξ_{po} = particle displacement outside the surface of a liner
ξ_0, η_0, ζ_0 = blade-fixed coordinate system for a source in the transformed space
ξ_{0m} = source coordinate for the mth blade
ρ = perturbation density
ρ_0 = mean density
σ = interblade phase angle
τ = time in a source point
Ω = rotating speed of rotor
ω = angular frequency
ω_b = perturbation frequency of blade force

Received 14 January 1999; revision received 15 February 2000; accepted for publication 28 February 2000.

*Visiting Professor, Department of Aeronautics and Astronautics; currently Professor, Department of Jet Propulsion, Beijing University of Aeronautics and Astronautics, 100083 Beijing, People's Republic of China.
†Professor, Department of Aeronautics and Astronautics.

I. Introduction

ALMOST all commercial aeroengines have a casing with acoustic treatment designed to reduce noise. An interesting problem is whether there is some possibility of designing casing treatment to suppress the blade flutter. As the first step toward dealing with the problem, it is clear that emphasis should be placed on elucidating how a nonrigid wall or soft wall affects the aeroelastic stability of a rotor. In fact, Watanabe and Kaji[1] and Namba et al.[2] have previously presented two different models to investigate the effects of wall admittance changes on aeroelastic stability of turbomachines. On the other hand, all numerical results from the models show that a nonrigid wall indeed has more or less influence on the unsteady pressure distribution and the aeroelastic stablity of blades, and there is some possiblity of suppresing blade flutter through a nonrigid wall under a given wall admittance. However, the exising models are for subsonic cascades, and an investigation related to a supersonic cascade with subsonic leading edge locus has not been attempted for a nonrigid wall until now. The latter may be more interesting for the practical application. Hence, the present analysis will focus on how to set up a model to investigate the effect of a nonrigid wall on flutter of supersonic cascades with subsonic leading-edge locus.

The boundary condition of a nonrigid wall takes effect on the flowfield or acoustic field theoretically by the variation of the eigenvalues. However, because the eigenfunctions no longer exhibit the orthogonality property for a lined duct containing uniform mean flow,[3,4] compared with the hard-wall case this will result in a great difficulty for the derivation of a Green's function required by setting up an upwash integral equation. Zorumski[4] presented an important clue to derive Green's function for a lined duct, in which the boundary condition is directly coupled with the basic equations by using Fourier transforms. This work has verified that there is a solution which consists of nonorthogonal eigenfunctions. In fact, the mode-matching approach widely used in duct acoustics is just based on this theoretical framework. Hence, in the present invetigation we find

such solutions by use of an effective mathematical tool. First, the double Fourier transform technique is applied to obtain the Green's function for a duct with an arbitrary locally reacting admittance on one wall, and then an upwash integral equation is derived by using generalized Green function theory and solving three-dimensional Euler equations with a given cascade geometry. By letting the wall admittance become zero, the hard-wall solution derived by the previous investigators is recovered. On the other hand, the eigenvalue equation describing the boundary condition has been transformed into a nonlinear ordinary equation,[5,6] which is then solved by a fourth-order Runge–Kutta scheme. The computed eigenvalues show very good agreement with the existing results for a nonrigid wall. Based on the preceding check, the calculation is then extended to investigate the effect of a nonrigid wall on the flow of a stator and rotor blade row. We have found that the change of wall admittance leads to very remarkable changes in the lift and moment coefficients and further in the aeroelastic stability of a blade row. Finally, the concluding remarks are given on the basis of the present theory and corresponding numerical simulation.

II. Mathematical Model

A. Basic Equations

The cascade flow model used in this analysis is shown in Fig. 1, all variables being physical or dimensional ones. Later scale lengths will be taken with respect to the semichord b for convenience. In addition, the following assumptions are made:

1) The system is three dimensional, which has a mean flow between two infinite parallel plates, as shown in Fig. 1. Especially, the lower plate (hub side) is assumed rigid, whereas the upper plate (tip side) is assumed to have a finite acoustic impedance.

2) The blades are flat plates of negligible thickness.

3) The mean angle of incidence is zero. There is no steady blade loading, and the mainstream flow passes through the cascade undeflected.

4) All perturbations from the uniform mean flow are small so that the flow equations can be linearized and the principle of superpostion can be applied to the solutions obtained.

5) The flow is supersonic with axial subsonic flow.

In addition to the preceding assumptions, when the wall admittance has a positive imaginary part an unsteady mode will be triggered, which is related to Helmholtz instability waves.[3,7] In the present analysis the effect of unstable surface modes will be ignored. So, the perturbation pressure p induced by the motion of the blade is then governed by the wave equation

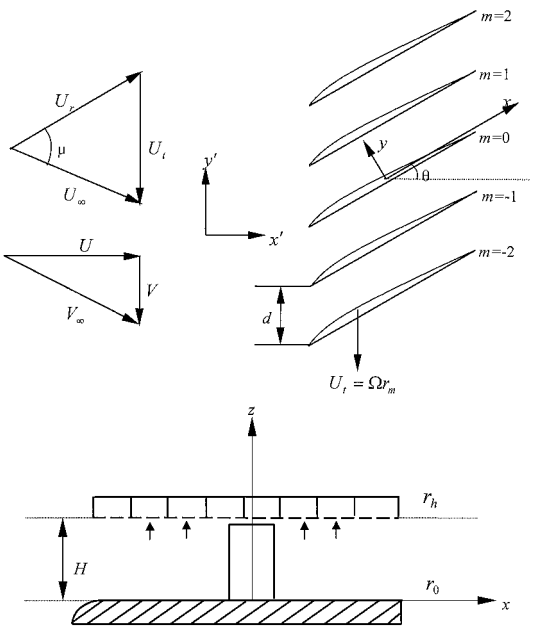

Fig. 1 Schematic of flow model.

$$\left(1 - M_r^2\right)\frac{\partial^2 p}{\partial x^2} + \frac{\partial^2 p}{\partial y^2} + \frac{\partial^2 p}{\partial z^2} - \frac{1}{a_0^2}\frac{\partial^2 p}{\partial t^2} - \frac{2M_r}{a_0}\frac{\partial^2 p}{\partial x \partial t} = 0 \quad (1)$$

where M_r is the mean flow Mach number in x direction as shown in Fig. 1, p is the fluctuating pressure, and a_0 is the velocity of sound.

The boundary condition is assumed to satisfy

$$\frac{\partial p}{\partial n} + b(\boldsymbol{y})p = a(\boldsymbol{y}, \tau) \quad \text{if} \quad \boldsymbol{y} \text{ on the tip side of duct}$$

$$\frac{\partial p}{\partial n} = 0 \quad \text{if} \quad \boldsymbol{y} \text{ on the hub side of duct} \quad (2)$$

where $a(\boldsymbol{y}, \tau)$ can be any function of $\boldsymbol{y}$ and τ (Ref. 8).

So, the Green's function of Eq. (1) satisfies

$$\left(1 - M_r^2\right)\frac{\partial^2 G}{\partial x_0^2} + \frac{\partial^2 G}{\partial y_0^2} + \frac{\partial^2 G}{\partial z_0^2} - \frac{1}{a_0^2}\frac{\partial^2 G}{\partial \tau^2} - \frac{2M_r}{a_0}\frac{\partial^2 G}{\partial x_0 \partial \tau}$$
$$= -\delta(t - \tau)\delta(\boldsymbol{x} - \boldsymbol{y}) \quad (3)$$

The corresponding boundary condition is

$$\frac{\partial G}{\partial n} + b(\boldsymbol{y})G = 0 \quad \text{if} \quad \boldsymbol{y} \text{ on the tip side of duct}$$

$$\frac{\partial G}{\partial n} = 0 \quad \text{if} \quad \boldsymbol{y} \text{ on the hub side of the duct} \quad (4)$$

According to the generalized Green's function theory,[8] the solution of Eq. (1) will be able to be expressed as

$$p(\boldsymbol{x}, t) = \int_{-T}^{T} \mathrm{d}\tau \int_A \left[G\left(\frac{\partial}{\partial n} + \frac{V_n}{a_0^2}\frac{\mathrm{D}_0}{\mathrm{D}\tau}\right)p(\boldsymbol{y}, \tau) \right.$$
$$\left. - p(\boldsymbol{y}, \tau)\left(\frac{\partial}{\partial n} + \frac{V_n}{a_0^2}\frac{\mathrm{D}_0}{\mathrm{D}\tau}\right)G(\boldsymbol{y}, \tau \mid \boldsymbol{x}, t) \right] \mathrm{d}S(\boldsymbol{y}) \quad (5)$$

B. Green's Function in a Lined Duct

Suppose G_ω represents the Fourier transforms of Green's Function in Eq. (3). Introducing the coordinate transforms $\xi = x/b$, $\eta = y\beta_r/b$, $\zeta = z\beta_r/b$ and then substituting $G_\omega = G'_\omega e^{-iKM_r\xi}$ into Eq. (3) yields[9]

$$G'_\omega = A\cos K_q\zeta_0 + B\sin K_q\zeta_0$$
$$- \frac{\exp\{-i[\omega t + (\alpha - KM_r)\xi + \beta\eta]\}}{bK_q}$$
$$\times \begin{cases} \cos K_q\zeta_0 \sin K_q\zeta, & \zeta_0 \le \zeta \\ \cos K_q\zeta \sin K_q\zeta_0, & \zeta_0 \ge \zeta \end{cases} \quad (6)$$

where

$$K = \omega b/a_0\beta_r^2 \quad (7)$$

$$\beta_r = \sqrt{M_r^2 - 1} \quad (8)$$

To determine the constants A and B, the concrete expression of the boundary condition defined in Eq. (2) is needed.

The liner can be modeled by a vortex sheet separating the uniform mean flow region within the duct from the no-flow region in the liner.[10] The impedance boundary condition is then applied on the no-flow side. The two regions are coupled by matching the pressure p and the particle displacement ξ_p. Further, from Eq. (6) the assumption can be made that the displacement be of the form

$$\xi_p = \xi_{\mathrm{pa}} \exp\{i[\omega\tau + (\alpha - KM_r)\xi_0 + \beta\eta_0]\} \quad (9)$$

However, if the relative movement between the wall and the blades is considered, a laboratory-fixed coordinates will have to be used. So, the following transforms are needed.

$$x = x' \cos\theta + (y' + \Omega r_m \tau)\sin\theta$$
$$y = -x' \sin\theta + (y' + \Omega r_m \tau)\cos\theta$$
$$z = z' \tag{10}$$

where r_m represents the mean radius of the rotor.

Substituting Eq. (10) into Eq. (9) yields

$$\xi_p = \xi_{pa} \exp[i(\omega'\tau + \alpha' x' + \beta' y')] \tag{11}$$

where

$$\alpha' = [(\alpha - KM_r)/b]\cos\theta - \beta(\beta_r/b)\sin\theta \tag{12}$$
$$\beta' = [(\alpha - KM_r)/b]\sin\theta + \beta(\beta_r b)\cos\theta \tag{13}$$
$$\omega' = \omega + (\beta' r_m)\Omega \tag{14}$$

With the pressure and displacement matching conditions on both sides of the liner,[10] one can see that

$$\frac{\beta_r}{b}\frac{\partial G_\omega}{\partial \zeta_0} + i\beta_a k_0' \left(1 + \frac{\alpha'}{k_0'}M_x - \frac{\beta'}{k_0'}M_y\right)^2 G_\omega = 0 \tag{15}$$

where

$$k_0' = \omega'/a_0 = [\omega + (\beta' r_m)\Omega]/a_0 \tag{16}$$

Let

$$\Delta_{\zeta_0}(G_\omega) = \frac{\beta_r}{b}\frac{\partial G_\omega}{\partial \zeta_0} + i\beta_a k_0' \left(1 + \frac{\alpha'}{k_0'}M_x - \frac{\beta'}{k_0'}M_y\right)^2 G_\omega \Big|_{\zeta_0 = h} = 0 \tag{17}$$

Because

$$\frac{\partial G}{\partial \zeta_0}\Big|_{\zeta_0 = 0} = 0 \tag{18}$$

by using the preceding two conditions, the constants A and B in Eq. (6) can be determined. Therefore the Green's function can be expressed as

$$G = \frac{1}{(2\pi)^3}\int_{-\infty}^{+\infty}\int_{-\infty}^{+\infty}\int_{-\infty}^{+\infty}\left[\frac{\cos K_q\zeta \cos K_q\zeta_0 \Delta_h(\sin K_q\zeta_0)}{bK_q\Delta_h(\cos K_q\zeta_0)} - \frac{1}{bK_q}\begin{cases}\cos K_q\zeta_0 \sin K_q\zeta, & \zeta_0 \le \zeta \\ \cos K_q\zeta \sin K_q\zeta_0, & \zeta_0 \ge \zeta\end{cases}\right] \times \exp[i\omega(\tau - t) + i(\alpha - KM_r)(\xi_0 - \xi) + i\beta(\eta_0 - \eta)]\,d\alpha\,d\beta\,d\omega \tag{19}$$

C. Derivation of Integral Equation

According to the boundary condition described in Eq. (17), the contribution from both upper and lower walls to the sound pressure in any point of the space surrounded by the walls will be zero. So, the only remaining contribution to produce sound pressure is related to the blade rows. Under such condition Eq. (5) will become

$$p(\boldsymbol{x}, t) = \int_{-T}^{T} d\tau \int_{A_{db}} \left(-p\frac{\partial G}{\partial n}\right) dS(\boldsymbol{y}) \tag{20}$$

where A_{db} is the periphery of a blade, which consists of the upper surface and the lower surface of a blade. Also, $\boldsymbol{n}$ is the normal to the surface A_{db} directed into the blade.

Assume the blade force changes with time dependence $\exp i\omega_b\tau$, i.e.,

$$\Delta p(\xi_0, \zeta_0, \tau) = \Delta\bar{p}(\xi_0, \zeta_0)e^{i\omega_b\tau} \tag{21}$$

hence

$$p(\boldsymbol{x}, t) = -\int_{-T}^{T} d\tau \int_{A_b} \Delta p(\xi_0, \zeta_0, \tau)\left(\frac{\beta_r}{b}\right)\frac{\partial G}{\partial \eta_0}\,dS(\boldsymbol{y}) \tag{22}$$

where Δp is the pressure difference between the lower and upper surface of a blade.

The theory of residues can be used to evaluate the inverse transforms of Eq. (22). In fact if $\Delta_h \cos K_q\zeta_0 = 0$, the poles in the β plane are, respectively,

$$\beta = \pm\sqrt{\alpha^2 - K_b^2 - K_q^2} \tag{23}$$

Then if $\zeta_0 - \zeta > 0$, a contour that circles the upper half of the β plane is used, and if $\zeta_0 - \zeta < 0$, a contour circling the lower half is used. In addition,

$$K_q\frac{\partial \Delta_h(\cos K_q\zeta_0)}{\partial\beta} = 2\beta\frac{\beta_r K_q h}{b\cos K_q}\left[\frac{1}{2}\left(1 + \frac{\sin 2K_q h}{2K_q h}\right) + \Lambda_1(\alpha, \beta) + \Lambda_2(\alpha, \beta)\right] \tag{24}$$

where

$$\Lambda_1(\alpha, \beta) = \frac{i\beta_a M_r}{\alpha h \beta_r}\left(1 + \frac{\alpha'}{k_0'}M_x - \frac{\beta'}{k_0'}M_y\right)\cos^2 K_q h \tag{25}$$

$$\Lambda_2(\alpha, \beta) = -\frac{i\beta_a M_t}{2\beta_r h}\left(1 + \frac{\alpha'}{k_0'}M_x - \frac{\beta'}{k_0'}M_y\right)^2 \times\left(\frac{\sin\theta}{\alpha} + \frac{\beta_r\cos\theta}{\beta}\right)\cos^2 K_q h \tag{26}$$

$$\Delta_h(\sin K_q\zeta_0) = \frac{\beta_r K_q}{b\cos K_q h} \tag{27}$$

So, Eq. (22) becomes

$$p(\boldsymbol{x}, t) = -\mathrm{sgn}(\eta - \eta_0)\frac{\beta_r}{4\pi b^2 h}\int_{A_b}\int_{-\infty}^{+\infty}\Delta\bar{p}(\xi_0, \zeta_0) \times\sum_{q=1}^{+\infty}\left\{\frac{\cos K_q\zeta \cos K_q\zeta_0}{\Lambda^{\pm}} \times\exp\left[i\omega_b t - i(\alpha + K_b M_r)(\xi - \xi_0) - i\sqrt{\alpha^2 - K_b^2 - K_q^2}|\eta - \eta_0|\right]\right\} d\alpha\,dS \tag{28}$$

where

$$\mathrm{sgn}(x) = \begin{cases}1, & x > 0 \\ -1, & x < 0\end{cases} \tag{29}$$

$$K_b = \omega_b b / a_0\beta_r^2 \tag{30}$$

$$\Lambda^{\pm} = \left[\frac{1}{2}\left(1 + \frac{\sin 2K_q h}{2K_q h}\right) + \Lambda_1(\alpha, \beta^{\pm}) + \Lambda_2(\alpha, \beta^{\pm})\right] \tag{31}$$

$$\beta^- = -\sqrt{\alpha^2 - K_b^2 - K_q^2} \tag{32}$$

$$\beta^+ = \sqrt{\alpha^2 - K_b^2 - K_q^2} \tag{33}$$

Let

$$\bar{p} = -\mathrm{sgn}(\eta - \eta_0)\frac{\beta_r}{4\pi b^2 h}\int_{A_b}\int_{-\infty}^{+\infty}\Delta\bar{p}(\xi_0,\zeta_0)$$
$$\times\sum_{q=1}^{+\infty}\left\{\frac{K_q\zeta\cos K_q\zeta_0}{\Lambda^{\pm}}\right.$$
$$\times\exp\left[-i(\alpha + K_bM_r)(\xi-\xi_0)\right.$$
$$\left.\left.-i\sqrt{\alpha^2 - K_b^2 - K_q^2}|\eta-\eta_0|\right]\right\}\mathrm{d}\alpha\,\mathrm{d}S \tag{34}$$

As shown in Fig. 1,

$$\xi_{0m} = \xi_0 + mh_1, \qquad m = 0, \pm1, \pm2, \ldots$$
$$\eta_{0m} = mh_2\beta_r, \qquad m = 0, \pm1, \pm2, \ldots \tag{35}$$

For mth blade

$$\bar{p}_m = -\mathrm{sgn}(\eta_m)\frac{\beta_r}{4\pi b^2 h}\int_{A_b}\int_{-\infty}^{+\infty}\sum_{q=1}^{+\infty}\frac{\cos K_q\zeta\cos K_q\zeta_0}{\Lambda^{\pm}}$$
$$\times\Delta\bar{p}_m(\xi_{0m},\zeta_{0m})\exp\left\{-i(\alpha+K_bM_r)[\xi-(\xi_0+mh_1)]\right.$$
$$\left.-i\sqrt{\alpha^2-K_b^2-K_q^2}|\eta-mh_2\beta_r|\right\}\mathrm{d}\alpha\,\mathrm{d}S \tag{36}$$

where

$$\eta_m = \eta - mh_2\beta_r \tag{37}$$

Assume

$$\Delta\bar{p}_m(\xi_{0m},\zeta_{0m}) = \Delta\bar{p}_0(\xi_0,\zeta_0)e^{im\sigma} \tag{38}$$

where σ is called the interblade phase angle. If the complete solution to Eq. (1) is expressed simply as a sum over all blades of function $\bar{p}_m$, then

$$\bar{p} = \sum_{m=-\infty}^{m=\infty}\bar{p}_m = -\frac{\beta_r}{4\pi b^2 h}\int_{-\infty}^{+\infty}\Delta\bar{p}_0(\xi_0,\zeta_0)$$
$$\times\sum_{q=1}^{+\infty}\left(\frac{\cos K_q\zeta\cos K_q\zeta_0}{\Lambda^{\pm}}\sum_{m=-\infty}^{m=\infty}\mathrm{sgn}(\eta_m)\right.$$
$$\times\exp\left\{im\sigma - i(\alpha+K_bM_r)[\xi-(\xi_0+mh_1)]\right.$$
$$\left.\left.-i\sqrt{\alpha^2-K_b^2-K_q^2}|\eta-mh_2\beta_r|\right\}\right)\mathrm{d}\alpha \tag{39}$$

Therefore, the corresponding upwash integral equation can be written as

$$\frac{\bar{v}(\xi,\eta,\zeta)}{U_r} = \int_0^1\int_{-1}^1 f(\xi_0,\zeta_0)K(\xi-\xi_0,\eta,\zeta\,|\,\zeta_0)\,\mathrm{d}\xi_0\,\mathrm{d}\zeta_0 \tag{40}$$

where

$$f(\xi_0,\zeta_0) = \frac{\Delta\bar{p}_0(\xi_0,\zeta_0)}{\rho_0U_r^2} \tag{41}$$

$$K(\xi-\xi_0,\eta,\zeta\,|\,\zeta_0) = \frac{i\beta_r}{4\pi}\frac{\partial}{\partial\eta}\int_{-\infty}^{+\infty}\sum_{q=1}^{+\infty}\left(\frac{\cos K_q\zeta\cos K_q\zeta_0}{\Lambda^{\pm}(\alpha+K_b/M_r)}\right.$$
$$\times\sum_{m=-\infty}^{m=\infty}\mathrm{sgn}(\eta_m)\exp\left\{im\sigma - i(\alpha+K_bM_r)[\xi-(\xi_0+mh_1)]\right.$$
$$\left.\left.-i\sqrt{\alpha^2-K_b^2-K_q^2}|\eta-mh_2\beta_r|\right\}\right)\mathrm{d}\alpha \tag{42}$$

By letting $\eta\to 0$, an integral equation for the pressure across the zeroth blade in terms of the known upwash velocity on the blade surface can be expressed as

$$\frac{\bar{v}(\xi,0,\zeta)}{U_r} = \int_0^1\int_{-1}^1 f(\xi_0,\zeta_0)K(\xi-\xi_0,\zeta\,|\,\zeta_0)\,\mathrm{d}\xi_0\,\mathrm{d}\zeta_0 \tag{43}$$

where

$$K(\xi-\xi_0,\zeta\,|\,\zeta_0) = \lim_{\eta\to 0}K(\xi-\xi_0,\eta,\zeta\,|\,\zeta_0) \tag{44}$$

It can be further shown that

$$K(\xi-\xi_0,\zeta\,|\,\zeta_0) = \frac{i\beta_r}{4\pi}\lim_{\eta\to 0}\frac{\partial}{\partial\eta}$$
$$\times\int_{-\infty}^{+\infty}\sum_{q=1}^{+\infty}\frac{\cos K_q\zeta\cos K_q\zeta_0\exp[-i(\alpha+K_bM_r)(\xi-\xi_0)]}{(\alpha+K_b/M_r)}$$
$$\times\frac{1}{2i}\left\{\frac{\exp\left[i\sqrt{\alpha^2-K_b^2-K_q^2}\,\eta\right]\exp[(i/2)\Delta_-]}{\Lambda^-\sin\frac{1}{2}\Delta_-}\right.$$
$$\left.+\frac{\exp\left(-i\sqrt{\alpha^2-K_b^2-K_q^2}\,\eta\right)\exp[(i/2)\Delta_+]}{\Lambda^+\sin\frac{1}{2}\Delta_+}\right\}\mathrm{d}\alpha \tag{45}$$

where

$$\Delta_- = (\Gamma + h_1\alpha) + h_2\beta_r\beta^- \tag{46}$$
$$\Delta_+ = (\Gamma + h_1\alpha) + h_2\beta_r\beta^+ \tag{47}$$
$$\Gamma = \sigma + K_bM_rh_1 \tag{48}$$

As discussed in Ref. 11, the integrand possesses only poles of the integrand at $\alpha_v = K_b/M_r$ and at the points where $\Delta_\pm = 2n\pi$ for $n = 0, \pm1, \pm2, \ldots$. But it follows from Eqs. (46) and (47) that the latter points are determined by

$$\alpha_n^{\pm} = -\left(\Gamma_nh_1/d^2\right) \pm (\beta_rh_2/d)\sqrt{(\Gamma_n/d)^2 - K_b^2 - K_q^2} \tag{49}$$

where

$$\Gamma_n = \Gamma - 2n\pi, \quad \text{for} \quad n = 0, \pm1, \pm2, \ldots \tag{50}$$
$$d = \sqrt{h_1^2 - h_2^2\beta_r^2} \tag{51}$$

When $\xi_0 - \xi < 0$, the contour must be closed in the lower half of the α plane and when $\xi_0 - \xi > 0$ in the upper plane. Upon evaluating the residues, for the vortex wave propagating downstream ($\xi_0 - \xi < 0$)

$$\alpha_v = -K_b/M_r \tag{52}$$

the corresponding kernel function can be expressed as

$$K(\xi-\xi_0,\zeta\,|\,\zeta_0) = \frac{\beta_r}{2}\sum_{q=1}^{+\infty}\frac{\cos K_{qv}\zeta\cos K_{qv}\zeta_0}{\Lambda_v}$$
$$\times\frac{\beta_v\sin(h_2\beta_r\beta_v)\exp[-i\left(\beta_r^2K_b/M_r\right)(\xi-\xi_0)]}{\cos(h_2\beta_r\beta_v) - \cos(\Gamma+\alpha_vh_1)} \tag{53}$$

where

$$\beta_v = \sqrt{\alpha_v^2 - K_b^2 - K_{qv}^2} \tag{54}$$

because the wavelength of the pressure wave and the vortex wave are different from each other. One can assume that the vortex wave will not be influenced by the wall admittance like the pressure wave. Because of this, it can be shown that

$$K_{qv} = \frac{\pi(q-1)}{h} = \frac{\pi(q-1)b}{H\beta_r}, \qquad q = 1, 2, 3, \ldots \tag{55}$$

$$\Lambda_v = \begin{cases} 1, & q = 1 \\ 0.5, & q \neq 1 \end{cases} \tag{56}$$

For the downstream pressure wave ($\xi_0 - \xi < 0$), the kernel function consisting of the convergent series[12] is

$$K(\xi - \xi_0, \zeta \mid \zeta_0) = \frac{\beta_r}{2} \sum_{q=1}^{+\infty} \frac{\cos K_{qv}\zeta \cos K_{qv}\zeta_0}{\Lambda_v}$$

$$\times \frac{\beta_v \sin(h_2\beta_r\beta_v)\exp\left[-i\left(\beta_r^2 K_b / M_r\right)(\xi - \xi_0)\right]}{\cos(h_2\beta_r\beta_v) - \cos(\Gamma + \alpha_v h_1)}$$

$$+ \frac{\beta_r^2 h_2}{2d^2} \sum_{n=-\infty}^{+\infty} \sum_{q=1}^{+\infty} \left(\frac{\cos K_q\zeta \cos K_q\zeta_0}{\Lambda\left(\alpha_n^+, \beta_n^-\right)} \right.$$

$$\times \frac{\left(\alpha_n^{+2} - K_b^2 - K_q^2\right)\exp\left[-i\left(\alpha_n^+ + K_b M_r\right)(\xi - \xi_0)\right]}{\left(\alpha_n^+ + \Gamma_n h_1 / d^2\right)\left(\alpha_n^+ + K_b / M_r\right)}$$

$$+ \frac{d^2 \cos K_q\zeta \cos K_q\zeta_0 \exp[-iK_b M_r(\xi - \xi_0)]}{\beta_r h_2(h_1 + \beta_r h_2)\Lambda_s}$$

$$\left. \times \exp\{i[\Gamma_n/(h_1 + \beta_r h_2)](\xi - \xi_0)\} \right)$$

$$- \sum_{q=1}^{+\infty} \sum_{n=-\infty}^{n=\infty} \frac{\beta_r \cos K_q\zeta \cos K_q\zeta_0}{2\Lambda_s}$$

$$\times \exp[in(\sigma - K_b M_r \beta_r h_2)]\delta(\xi - \xi_0 - nd_1) \tag{57}$$

where

$$\Lambda\left(\alpha_n^+, \beta_n^-\right) = \left[\frac{1}{2}\left(1 + \frac{\sin 2K_q h}{2K_q h}\right) \right.$$

$$\left. + \Lambda_1\left(\alpha_n^+, \beta_n^-\right) + \Lambda_2\left(\alpha_n^+, \beta_n^-\right) \right] \tag{58}$$

$$\alpha_n^+ = -\Gamma_n h_1 / d^2 + (\beta_r h_2 / d)\sqrt{(\Gamma_n/d)^2 - K_b^2 - K_q^2} \tag{59}$$

$$\beta_n^- = \Gamma_n h_2 \beta_r / d^2 - (h_1/d)\sqrt{(\Gamma_n/d)^2 - K_b^2 - K_q^2} \tag{60}$$

$$\alpha_n^{+\prime} = \left(1/\beta_0^2\right)\left\{-M_x K_t + \sqrt{K_t^2 - \beta_0^2\left[\left(\beta_n^{-\prime}\right)^2 + K_q^{2\prime}\right]}\right\} \tag{61}$$

$$K_t = k_b' - (\sigma - 2\pi n)M_y/d' \tag{62}$$

$$k_b' = k_b + (\sigma - 2\pi n)M_t/d' \tag{63}$$

$$\beta_n^{-\prime} = -(\sigma - 2\pi n)/d' \tag{64}$$

$$d' = b\sqrt{h_1^2 + h_2^2} \tag{65}$$

$$K_q' = (\beta_r/b)K_q \tag{66}$$

$$\Lambda_s = \begin{cases} 1, & q = 1 \\ 0.5, & q \neq 1 \end{cases}$$

$$d_1 = h_1 + h_2\beta_r \tag{67}$$

$$d_2 = h_1 - h_2\beta_r \tag{68}$$

For the upstream pressure wave ($\xi_0 - \xi > 0$), the kernel function is

$$K(\xi - \xi_0, \zeta \mid \zeta_0) = -\frac{\beta_r^2 h_2}{2d^2} \sum_{n=-\infty}^{+\infty} \sum_{q=1}^{+\infty} \left(\frac{\cos K_q\zeta \cos K_q\zeta_0}{\Lambda\left(\alpha_n^+, \beta_n^-\right)} \right.$$

$$\times \frac{\left(\alpha_n^{+2} - K_b^2 - K_q^2\right)\exp\left[-i\left(\alpha_n^+ + K_b M_r\right)(\xi - \xi_0)\right]}{\left(\alpha_n^+ + \Gamma_n h_1 / d^2\right)\left(\alpha_n^+ + K_b / M_r\right)}$$

$$- \frac{d^2 \cos K_q\zeta \cos K_q\zeta_0 \exp[-iK_b M_r(\xi - \xi_0)]}{\beta_r h_2(h_1 - \beta_r h_2)\Lambda_s}$$

$$\left. \times \exp\{i[\Gamma_n/(h_1 - \beta_r h_2)](\xi - \xi_0)\} \right)$$

$$- \sum_{q=1}^{+\infty} \sum_{n=-\infty}^{n=\infty} \frac{\beta_r \cos K_q\zeta \cos K_q\zeta_0}{2\Lambda_s}$$

$$\times \exp[in(\sigma + K_b M_r \beta_r h_2)]\delta(\xi - \xi_0 - nd_2) \tag{69}$$

where

$$\Lambda\left(\alpha_n^-, \beta_n^+\right) = \left[\frac{1}{2}\left(1 + \frac{\sin 2K_q h}{2K_q h}\right) + \Lambda_1\left(\alpha_n^-, \beta_n^+\right) \right.$$

$$\left. + \Lambda_2\left(\alpha_n^-, \beta_n^+\right) \right] \tag{70}$$

$$\alpha_n^- = -\Gamma_n h_1 / d^2 - (\beta_r h_2/d)\sqrt{(\Gamma_n/d)^2 - K_b^2 - K_q^2} \tag{71}$$

$$\beta_n^+ = \Gamma_n h_2 \beta_r / d^2 + (h_1/d)\sqrt{(\Gamma_n/d)^2 - K_b^2 - K_q^2} \tag{72}$$

$$\alpha_n^{-\prime} = \left(1/\beta_0^2\right)\left\{-M_x K_t - \sqrt{K_t^2 - \beta_0^2\left[\left(\beta_n^{+\prime}\right)^2 + K_q^{2\prime}\right]}\right\} \tag{73}$$

$$\beta_n^{+\prime} = -(\sigma - 2\pi n)/d' \tag{74}$$

III. Numerical Example and Discussion

A. Eigenvalue Equation

As just indicated, the eigenvalues of Eq. (19) will be given by

$$\Delta_h(\cos K_q\zeta_0) = 0 \tag{75}$$

For soft walls with rotor-blade rows, Eq. (75) can be derived as

$$\left(\frac{K_q'}{k_0'}\right)\tan k_0' H\left(\frac{K_q'}{k_0'}\right) = i\beta_a\left(1 + \frac{\alpha'}{k_0'}M_x - \frac{\beta'}{k_0'}M_y\right)^2 \tag{76}$$

One considers the eigenvalue K_q'/k_0' to be a fucntion of some parameter η_z. Assume β_a to be a function of this parameter. If Eq. (76) is differentiated with respect to η_z, then the following single ordinary differential equation results:

$$\frac{\partial}{\partial\eta_z}\left(\frac{K_q'}{k_0'}\right) = \frac{i\beta_{af}[1 + (\alpha'/k_0')M_x - (\beta'/k_0')M_y]^2}{A_{ts} + 2i\beta_a(\eta_z)[1 + (\alpha'/k_0')M_x - (\beta'/k_0')M_y]A_p} \tag{77}$$

where

$$A_p = \frac{\pm M_x(K_q'/k_0')}{\sqrt{(K_t/k_0')^2 - \beta_0^2\left[(\beta'/k_0')^2 + (K_q'/k_0')^2\right]}} \tag{78}$$

$$A_{ts} = \left[\tan k_0' H\left(\frac{K_q'}{k_0'}\right) + k_0' H\left(\frac{K_q'}{k_0'}\right)\sec^2 k_0' H\left(\frac{K_q'}{k_0'}\right) \right] \tag{79}$$

On the other hand, the preceding equations have used the expression $\beta_a(\eta_z) = \eta_z\beta_{af}$, $0 < \eta_z < 1$. Therefore, if Eq. (77) is integrated on $0 < \eta_z < 1$, a hard-wall eigenvalue being used as the initial value, then at $\eta_z = 1$ the solution to Eq. (77) will be an eigenvalue for the condition β_{af}.

B. Solution of Integral Equation

Consider the integral equation given by

$$\frac{\bar{v}(\xi, \zeta)}{U_r} = \int_0^1 \int_{-1}^1 f(\xi_0, \zeta_0) K(\xi - \xi_0, \zeta \,|\, \zeta_0)\, \mathrm{d}\xi_0\, \mathrm{d}\zeta_0 \qquad (80)$$

When the kernel functions given by Eqs. (57) and (69) are substituted into Eq. (81), a functional integral equation can be obtained from the introduction of terms of the form $\Delta p(x + nd_{1,2})$ caused by the integration of the delta functions. On the other hand, these terms will make it difficult to obtain accurate numerical results by directly solving the equation. However, a similar method suggested by Nagashima and Whitehead[13] and Ni[14] can be used to overcome the difficulty, i.e., a new dipole strengh is defined along the chord of the reference blade in order to give the required Mach wave reflections explicitly, and then the method of collocation can be used to solve the integral equation.

C. Comparison with Compressible Results with Hard Walls

When the wall admittance tends to zero, one of the theoretical results in the present analysis is the upwash velocity integral equation with kernel function for a hard-wall case. At the same time the radial standing wave will have no contribution to the integration of blade pressure distribution. So, in this case the conclusion can be made that the result of solving the three-dimensional integral equation for a hard wall will reduce to that from the two-dimensional model if the blade lift and moment coefficients are defined as

$$C_{Fq} = \frac{1}{\rho_0 U_r \bar{v}_b H b} \int_0^1 \int_0^\pi \Delta \bar{p}(\xi_0, \zeta_0)\, \mathrm{d}\xi_0\, \mathrm{d}\zeta_0 \qquad (81)$$

$$C_{Mq} = \frac{1}{\rho_0 U_r \bar{v}_b H b^2} \int_0^1 \int_0^\pi \xi_0 \Delta \bar{p}(\xi_0, \zeta_0)\, \mathrm{d}\xi_0\, \mathrm{d}\zeta_0 \qquad (82)$$

for a bending vibration, and

$$C_{F\alpha} = \frac{1}{\rho_0 U_r^2 \alpha_t H b} \int_0^1 \int_0^\pi \Delta \bar{p}(\xi_0, \zeta_0)\, \mathrm{d}\xi_0\, \mathrm{d}\zeta_0 \qquad (83)$$

$$C_{M\alpha} = \frac{1}{\rho_0 U_r^2 \alpha_t H b^2} \int_0^1 \int_0^\pi \xi_0 \Delta \bar{p}(\xi_0, \zeta_0)\, \mathrm{d}\xi_0\, \mathrm{d}\zeta_0 \qquad (84)$$

for a torsional vibration, where $\bar{v}_b$ represents the amplitude of upwash velocity caused by bending vibration and α_t is the amplitude of the angular displacement caused by torsional vibration of a blade.

According to the preceding definition, Tables 1 and 2 give the results of solving the present three-dimensional integral equation and those from Refs. 13–16. These results show very good agreement between each other.

D. Numerical Results for a Rotor-Blade Row

As has been indicated, if the incoming velocity U_r along the chordwise direction and other geometrical conditions remain the same the upwash integral equation for both a stator-blade row and a rotor-blade row with a hard wall will have the same expression. However, for a soft wall their integral equations will have two differences. First, there is an additional term for the expression of kernel function of a rotor-blade row, which is related to the circumferential Mach number M_t of the blade. Second, the transformation between a duct-fixed coordinate and a blade-fixed coordinate will lead to a shift of perturbation frequency of the blade. This means that the real frequency interacting with the wall will be different from that for a stator-blade row. In fact, it can be shown from Eq. (63) that

$$\omega_t = \omega_b + B_r(\sigma' - n)\Omega, \qquad n = 0, \pm 1, \pm 2, \ldots \qquad (85)$$

where $\sigma' = \sigma/2\pi$ and B_r is the blade number of the rotor.

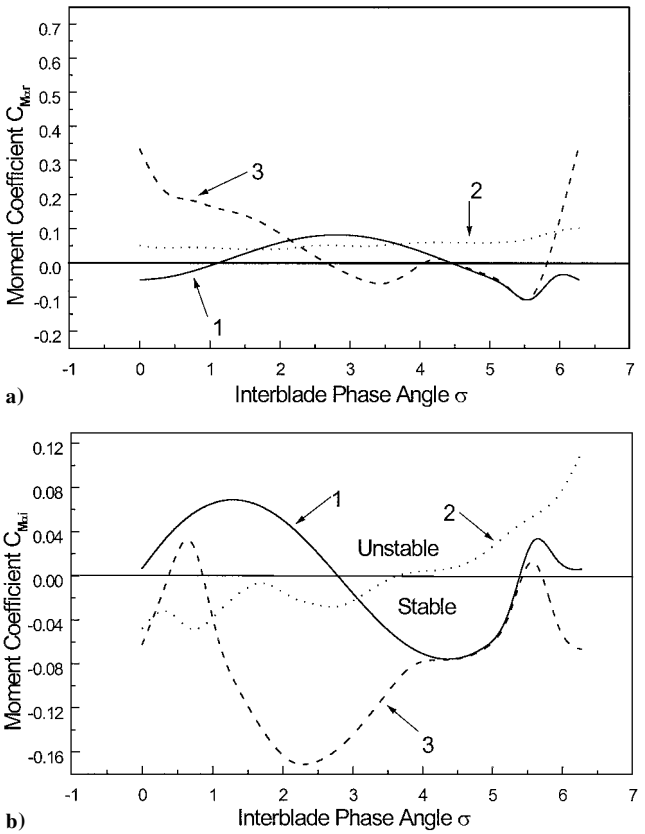

Fig. 2 Effect of interblade phase angle on the moment coefficient caused by torsional motion under various wall admittance: 1, hard wall; 2, soft wall $\beta_a = (0.10, -0.18)$; 3, soft wall $\beta_a = (0.2, 0.10)$. Also $\lambda = 0.301$, $\theta = 59.93$, space/chord = 0.7889, span/chord = 4.0, $M_r = 1.3454$, $M_t = 1.36$. These coefficients are referred to an axis position at the midchord point.

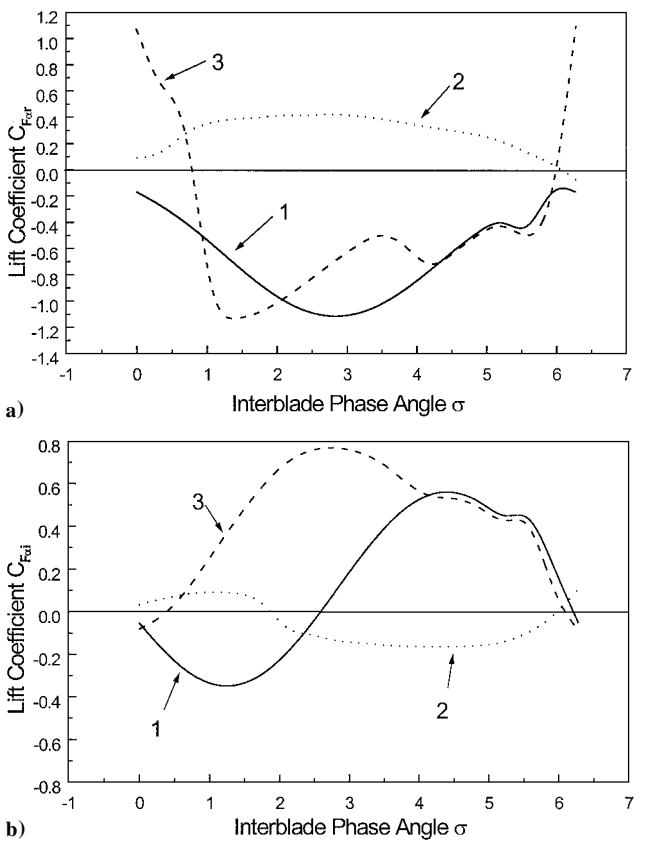

Fig. 3 Effect of interblade phase angle on the lift coefficient caused by torsional motion under various wall admittance. The other conditions are the same as in Fig. 2.

Table 1 Lift and moment coefficients

	Bending		Torsion	
λ	C_{Fq}	C_{Mq}	$C_{F\alpha}$	$C_{M\alpha}$
0.301	$-0.1592+i0.3822$	$-0.0241+i0.0648$	$-0.1396+i0.3894$	$-0.0181+i0.0417$
——	$-0.1592+i0.3822$	$-0.0239+i0.0649$	$-0.1397+i0.3894$	$-0.0179+i0.0418$

Note: The first row gives results from Ref. 13 for a given reduced frequence λ; the second row is the results of the present program. $\theta = 59.53$, $\sigma = -30$, $M_r = 1.3454$, space/chord = 0.7889.

Table 2 Moment coefficient $C_{M\alpha}$

σ	Present analysis	Adamcyk's analysis	Verdon's analysis
−180.0000	$0.5259-i0.3718$	$0.5212-i0.3641$	$0.51-i0.37$
−150.0000	$0.3330-i0.5107$	$-0.3309-i0.5030$	$-0.34-i0.5$
−120.0000	$0.0848-i0.5225$	$0.08566-i0.5153$	$0.11-i0.57$
−90.0000	$-0.1819-i0.3969$	$-0.1790-i0.3910$	$0.175-i0.408$
−60.0000	$0.1534-i0.2917$	$0.1617-i0.2895$	$0.160-i0.290$
−30.0000	$-0.190-i0.2840$	$-0.1872-i0.2824$	$-0.190-i0.28$
0.0000	$-0.2375+i0.0529$	$-0.2354+i0.5372$	$-0.24+i0.04$
30.0000	$-0.0552+i0.2603$	$-0.05435+i0.2602$	$-0.04+i0.26$
60.0000	$0.1859+i0.3257$	$0.1851+i0.3257$	$0.19+i0.30$
90.0000	$0.4161+i0.2560$	$0.4123+i0.2567$	$0.405+i0.24$
120.0000	$0.5725+i0.0782$	$0.5674+i0.08128$	$0.58+i0.05$
150.0000	$0.6134-i0.1534$	$0.6073-i0.1479$	$0.60-i0.16$
180.0000	$0.5256-i0.3716$	$0.5212-i0.3641$	$0.51-i0.37$

Note: The preceding results of both third and fourth column are all taken from Table 1 Verdon's cascade A in Ref. 15. Also $\lambda = 0.602$, $\theta = 59.53$, $M_r = 1.3454$, space/chord = 0.7889.

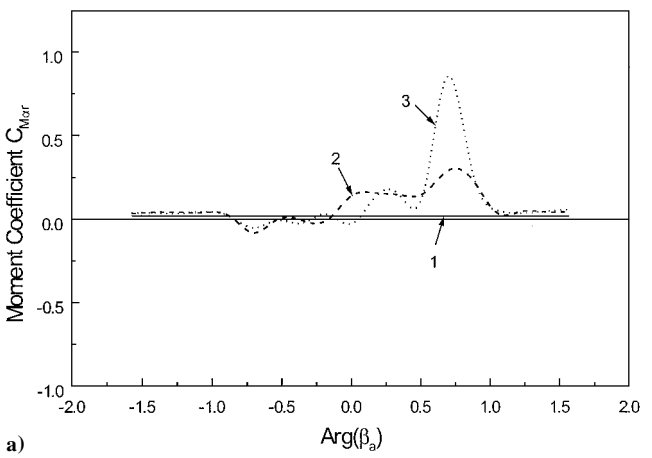

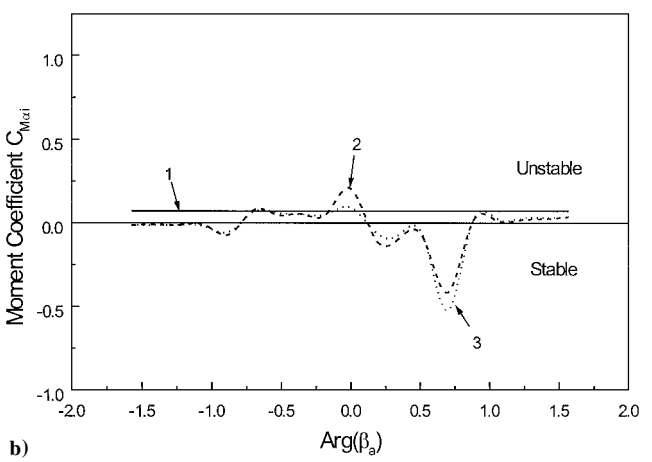

Fig. 4 Variation of moment coefficient caused by torsional motion with wall admittance: 1, hard wall $|\beta_a| = 0$; 2, soft wall $|\beta_a| = 0.2$; 3, soft wall $|\beta_a| = 0.6$. Also $\sigma = 1.39$, $\lambda = 0.301$, $\theta = 59.53$, space/chord = 0.7889, span/chord = 4.0, $M_r = 1.3454$, $M_t = 1.36$. These coefficients are referred to an axis position at the midchord point.

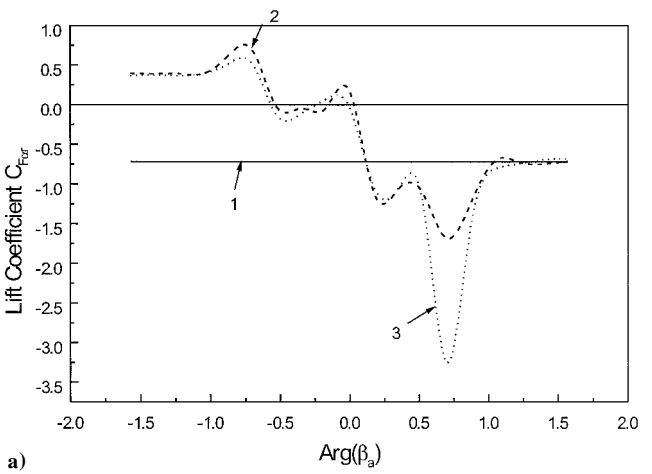

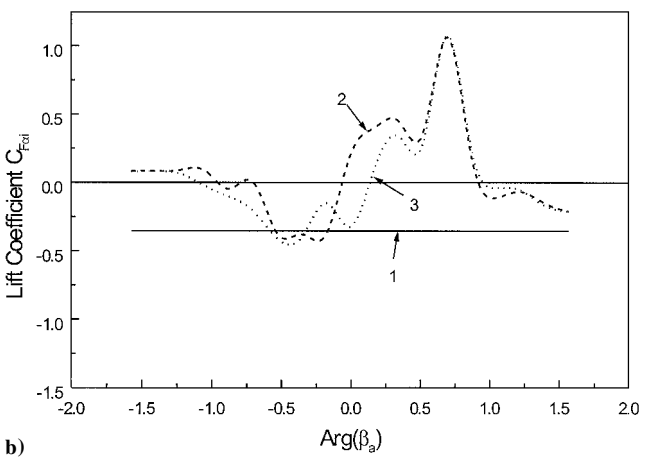

Fig. 5 Variation of lift coefficient caused by torsional motion with wall admittance. The other conditions are the same as in Fig. 4.

Equation (85) shows that the frequency in a duct-fixed coordinate depends not only the speed of rotor Ω but also on the interblade phase angle σ. Perhaps the most important feature from this expression is that for a stator-blade row, all modes interact with the wall at the same frequency, whereas for a rotor-blade row each mode has its own frequency that corresponds to a different mode number n shown in Eq. (85). Hence, for a rotor-blade row it will be unreasonable to assume that the wall has the same admittance for all modes. Actually, this means that if one hopes to control the aeroelastic stability of a given blade row through the wall it must be designed to have the required frequency response for each mode, at least for some main or key modes, to affect the blade aerodynamic loading. As a theoretical analysis, Figs. 2–7 give the results under the assumption that if circumferential mode number $|n| \leq 10$ β_a has a given value, otherwise $\beta_a = 0$. First, the moment and lift coefficients are plotted as a function of interblade phase angle in Figs. 2 and 3. Perhaps the most striking feature of these plots is that the change of wall admittance will also lead to a very prominent effect on the moment and lift coefficients of a supersonic cascade with subsonic leading-edge locus just as has been shown in a subsonic case.[1,2] Further, the imaginary part of the moment coefficient $C_{M\alpha i}$ will determine whether the blade flutters or not, i.e., if $C_{M\alpha i} < 0$, the system is stable; otherwise

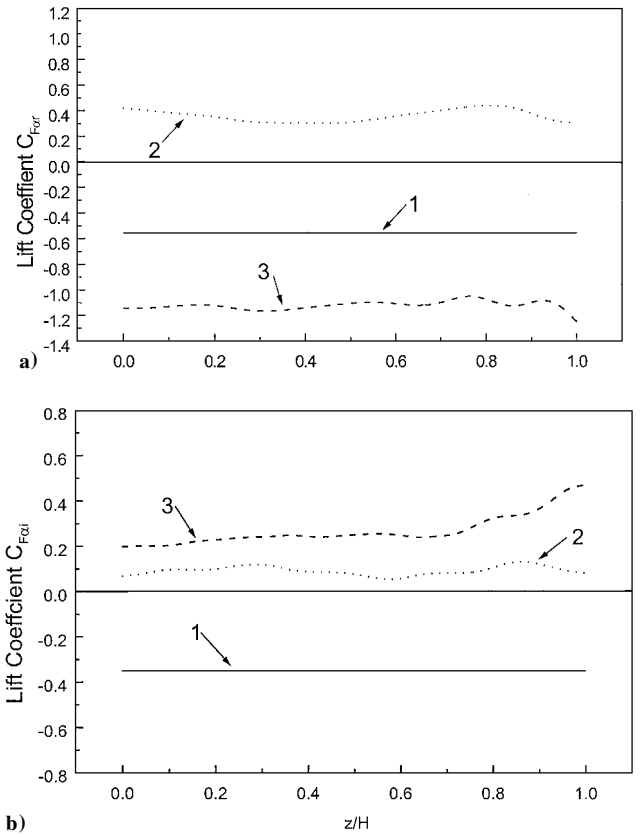

Fig. 6 Lift coefficient along the span: 1, hard wall; 2, soft wall β_a = (0.10, − 0.18); 3, soft wall β_a = (0.2, 0.10). Also σ = 1.39. The other conditions are the same as in Fig. 1.

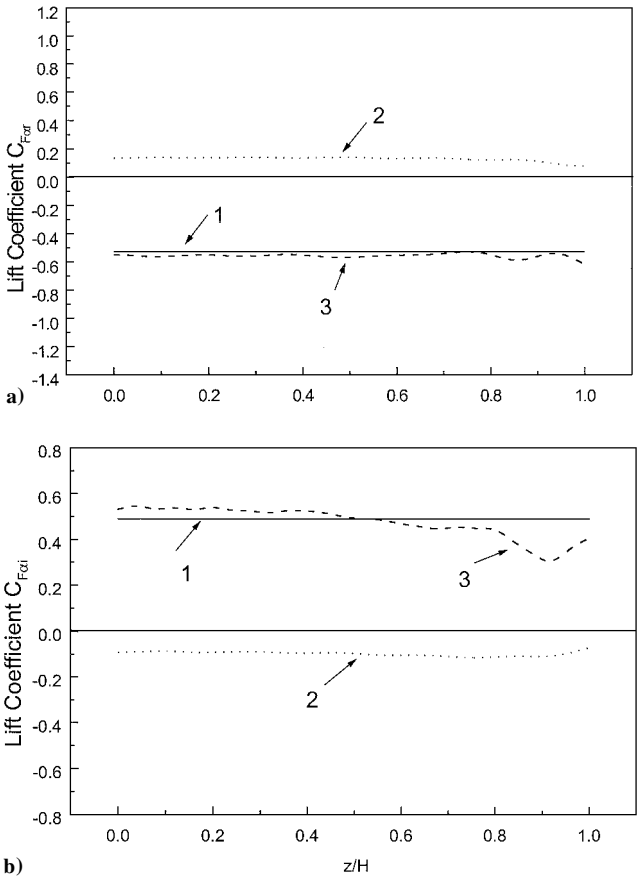

Fig. 7 Lift coefficient along the span: 1, hard wall; 2, soft wall β_a = (0.10, − 0.18); 3, soft wall β_a = (0.2, 0.10). Also σ = 5.58. The other conditions are the same as in Fig. 1.

it is unstable. Figure 2 shows the effect of interblade phase angle on the aeroelastic stability of a given blade row under various wall admittances. For a hard-wall case, plotted here with a solid line, the blade is unstable when the interblade phase angle ranges between 0 and π. But the blade is stable in this range for a given wall admittance value $\beta_a = (0.10, -0.18)$. In particular, when $\beta_a = (0.2, 0.1)$ the blade will remain stable for almost all interblade phase angle values except for very few points shown in Fig. 2b. However, the opposite results can be also found when the interblade phase angle varies from π to 2π for curve 2 with $\beta_a = (0.10, -0.18)$. Actually this means that for any given cascade whether soft walls will enhance the aeroelastic stability of the blade or not will depend on the wall admittance values. On the other hand, Fig. 2 also shows the most unstable point corresponds to the interblade phase angle $\sigma = 1.39$, which has its maximum positive moment coefficient $C_{M\alpha i} = 0.0707$. It may be very meaningful to know how this critical point responds to the wall admittance. In fact, Figs. 4 and 5 show the variation of the lift and moment coefficient with the wall admittance. In these two plots the wall admittance is expressed by its absolute value and argument and especially the latter is taken as an independent variable. There are some combinations that enable the blade to be stable for $|\beta_a| = 0.2$ and 0.6. These plots also clearly indicate that even though a few modes are controlled through the wall it is still found that the lift, moment coefficients, and stability will all be changed prominently compared with the results for the hard-wall case. Figures 6 and 7 give the lift coefficient along the span for two different interblade phase angles, which provide us with more detailed information about how the soft walls change the blade pressure distribution.

IV. Conclusions

In the present investigation a kind of new lifting surface model has been suggested based on the application of generalized Green's funtion theory and double Fourier transformation technique; the model is suitable for a supersonic cascade with subsonic leading-edge locus. The change of wall boundary conditions not only affects the eigenvalues of the system but also the eigenfunction normalizing factor in comparison with a rigid boundary condition, and it is these variations that finally influence the flow and acoustic fields. On the other hand, under a nonrigid boundary condition the kernel function expression for a rotor-blade row is different from that for a stator-blade row because of the motion and boundary condition effect, whereas under a rigid boundary condition these expressions can be reduced to the same results as that given in the preceding models. This provides a further check of the theoretical results. In fact, the moment and lift coefficients calculated by the present program show good agreement with those available in the literature for a hard-wall case. Based on the preceding check, the calculation is then extended to investigate the effect of a nonrigid wall on the flow of a rotor-blade row. The change of wall admittance leads to large changes in the lift and moment coefficients, a result which is quite similar to the analysis in a subsonic case. Perhaps the most important conclusion drawn from the present investigation is that whether a nonrigid wall has a positive effect on suppressing blade flutter will depend mainly on what admittance value the wall possesses. One of the best ways to suppress cascade blade flutter by use of a nonrigid wall is to find a soft wall with a controllable acoustic admittance. To realize the objectives, it is very apparent that considerable research effort is still requried.

Acknowledgments

The work described here was carried out while X. Sun was in receipt of a Japan Society for the Promotion of Science Fellowship, and the author is indebted to T. Watanabe at the University of Tokyo for many helpful discussions.

References

[1]Watanabe, T., and Kaji, S., "Possibility of Cascade Flutter Suppression by Use of Non-Rigid Duct Wall," *Proceedings of the Third International Symposium on Aeroelasticity in Turbomachines*, edited by P. S. Whitehead, Cambridge Univ., Cambridge, England, U.K., 1984, pp. 261–276.

[2]Namba, M., Yamsaki, N., and Kurihara, Y., "Some Three-Dimensional Effects on Unsteady Aerodynamic Forces on Oscillating Cascades,"

Proceedings of the Third International Symposium on Aeroelasticity in Turobomachines, edited by P. S. Whitehead, Cambridge Univ., Cambridge, England, U.K., 1984, pp. 217–230.

[3]Tester, B. J., "The Propagation and Attenuation of Sound in Lined Ducts Containing Uniform or Plug Flow," *Journal of Sound and Vibration*, Vol. 28, No. 2, 1973, pp. 151–203.

[4]Zorumski, W. E., "Acoustic Theory of Axisymmetric Multisectioned Ducts," NASA TR R-419, May 1974.

[5]Eversman, W., "Computation of Axial and Transveres Wave Numbers for Uniform Two-Dimensional Ducts with Flow Using a Numerical Integration Scheme," *Journal of Sound and Vibration*, Vol. 41, No. 2, 1975, pp. 252–255.

[6]Eversman, W., "Initial Values for the Integration Scheme to Compute the Eigenvalues for Propagation in Ducts," *Journal of Sound and Vibration*, Vol. 50, No. 1, 1977, pp. 159–162.

[7]Rienstra, S. W., "Hydrodynamic Instabilities and Surface Waves in a Flow over an Impedance Wall," *Aero- and Hydro-Acoustics IUTAM Symposium*, edited by G. Come-Bellot and J. E. Ffowcs Williams, Springer-Verlag, Lyon, France, 1986, pp. 483–490.

[8]Goldstein, M., *Aeroacoustics*, McGraw–Hill, New York, 1976, pp. 28, 29.

[9]Morse, P. M., and Feshbach, H., *Methods of Theoretical Physics*, Pt. I, McGraw–Hill, New York, 1953, pp. 791–895.

[10]Ko, S.-H., "Sound Attenuation in Acoustically Lined Circular Ducts in the Presence of Uniform Flow and Shear Flow," *Journal of Sound and Vibration*, Vol. 22, No. 2, 1973, pp. 193–210.

[11]Goldstein, M., "Cascade with Subsonic Leading-Edge Locus," *AIAA Journal*, Vol. 13. No. 8, 1975, pp. 1117–1119.

[12]Lighthill, M. J., *Fourier Analysis and Generalized Functions*, Cambridge Univ. Press, New York, 1958, p. 67.

[13]Nagashima, T., and Whitehead, D. S., "Linearized Supersonic Unsteady Flow in Cascades," Aeronautical Research Council, Repts. and Memoranda 3811, Feb. 1978.

[14]Ni, R. H., "A Rational Analysis of Periodic Flow Perturbation in Supersonic Two-Dimensional Cascade," *Journal of Engineering for Power*, Vol. 101, July 1979, pp. 431–438.

[15]Adamczyk, J. J., and Goldstein, M., "Unsteady Flow in a Supersonic Cascade with Leading-Edge Locus," *AIAA Journal*, Vol. 16. No. 12, 1978, pp. 1248–1254.

[16]Verdon, J. M., "Further Developments in the Aerodynamic Analysis of Unsteady Supersonic Cascades," *Journal of Engineering for Power*, Pt. 1, Pt. 2, Vol. 509, Oct. 1977, pp. 509–525.

P. J. Morris
Associate Editor